Bispectrum analysis of fluctuation of nanoparticle amount in amplitude modulated capacitively-coupled discharge plasmas

Masaharu Shiratani[1], Teppei Ito[1], Kazunori Koga[1], Masahiro Soejima[1], Daisuke Yamashita[1], Hyunwoong Seo[1], Naho Itagaki[1], Tatsuya Kobayashi[2], and Shigeru Inagaki[3]
siratani@ed.kyushu-u.ac.jp
[1] *Department of Electronics, Faculty of Information Science and Electrical Engineering, Kyushu University 744 Motooka, Nishi-ku, Fukuoka, 819-0395, Japan*
[2] *National Institute for Fusion Science, 322-6, Oroshi-cho, Toki-city, 509-5292, Japan*
[3] *Reserch Institute for Applied Mechanics, Kyushu University, 6-1 Kasuga-Koen, Kasuga-city, 816-8580, Japan*

Spatiotemporal evolution of nanoparticle amount in amplitude modulated capacitively-coupled discharge plasmas has been analysed using bispectral analysis to study interactions between plasmas and nanoparticles. Subharmonics of amplitude modulation frequency exit in the power spectra. Total bicoherence spectrum indicates nonlinear coupling between plasmas and nanoparticles.

1. Introduction

Understanding interactions between plasmas and nanomaterials is crucial for plasma nanoprocesses for nanodevices and nanomaterials because plasma fluctuation affects significantly their structure and properties [1, 2]. To study such interactions, we have employed nanoparticles grown in reactive plasmas[3-7]. Recently, we have found that applying amplitude modulation (AM) to discharge voltage suppresses growth of nanoparticles [8-11]. These results indicate radical density perturbation by AM discharges interacts with nanoparticle growth. Here we have analysed spatiotemporal evolution of nanoparticle amount in reactive plasmas using bispectral analysis to study interactions between plasmas and nanoparticles.

2. Experimental

Experiments were carried out using a capacitively-coupled parallel plate discharge plasma reactor equipped with a two-dimensional laser light scattering (LLS) system as shown in Fig. 1 [12-15]. The discharge was maintained between two electrodes separated by a distance of 20 mm. The lower electrode was a powered electrode of 60 mm in diameter and the upper one was a grounded electrode of 60 mm in diameter. Ar diluted $Si(CH_3)_2(OCH_3)_2$ (DM-DMOS) was introduced into the reactor. The flow rate of Ar and DM-DOMS were 40 sccm and 0.2 sccm, respectively. The total gas pressure was 1.25 Torr. To generate nanoparticles, we applied high frequency voltage of 60 MHz for 8 s between the two electrodes. The discharge voltage was 120 V, which corresponds to the power of 30 W. For the amplitude modulation experiments, AM frequency f_{AM} was 100 Hz and the AM level was 30%.

To obtain information on size, density, and motion of nanoparticles in plasmas, we measured optical emission intensities. A sheet of laser beam (λ= 532 nm and 2 W) was irradiated between the powered electrode and the grounded electrode. We measured LLS intensity (nanoparticle amount) of 90° Rayleigh scattering from nanoparticles using a high speed camera (Photoron FASTCAM SA4) equipped with an interference filter of a center wavelength of 532 nm with 1 nm FWHM, at a frame rate of 1000 fps.

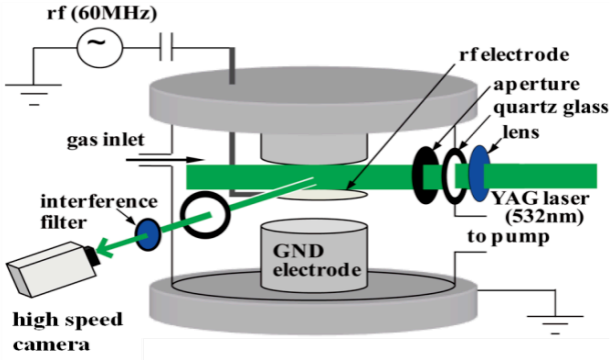

Fig. 1. Experimental setup.

To obtain information on radical generation rate and radical density, we measured optical emission intensities. The camera was also used for measurements of optical emission intensities from plasmas using interference filters of a center wavelength of 750 nm and 810 nm with 10 nm FWHM. We measured two-dimensional profiles of optical emission intensities from Ar I lines of 750.4 nm and 811.5 nm. The ratio of the emission intensities indicates Ar metastable density [6-7]. We employed the ratio as an indicator of radical density.

3. Results and discussion

Figure 2 shows time evolution of the spatial profiles of LLS intensity between the center of electrode (r = 0 mm). At 3s, most nanoparticles are located around the plasma/sheath boundary near the powered electrode (z~2mm) where nanoparticles were mainly generated and grow as shown Fig. 2(a).

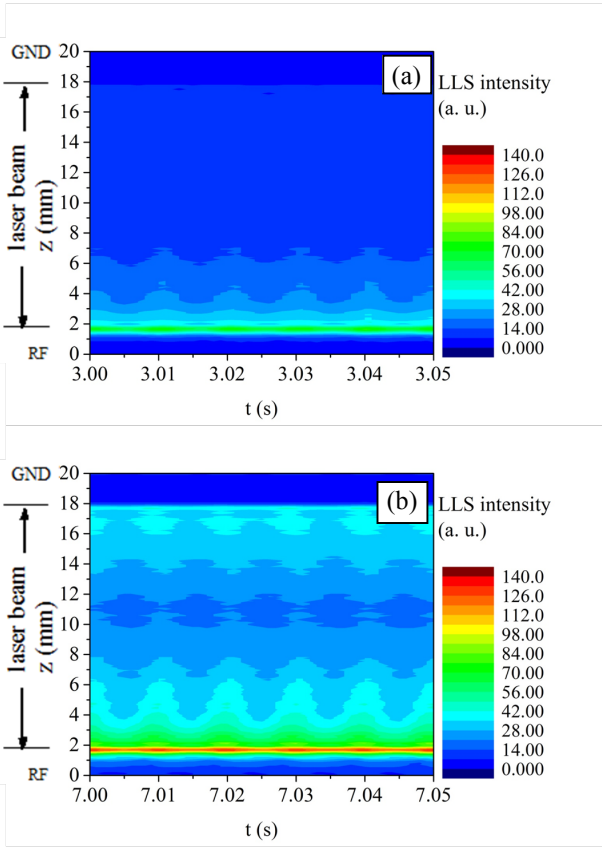

Fig. 2. Time evolution of the spatial profiles of LLS intensity during (a) t = 3-3.05 s, (b) t = 7-7.05 s.

The LLS intensity extends spatially toward the upper grounded electrode with time, and it reaches the plasma/sheath boundary near the upper grounded electrode around t = 7 s as shown in Fig. 2(b). The LLS intensity oscillates at the AM frequency (f_{AM} = 100 Hz). The oscillation of the nanoparticle amount around z= 10 mm in the plasma bulk shows phase delay compared with those around the plasma/sheath boundaries near the powered and grounded electrode.

Figure 3 shows time evolution of the spatial profiles of optical emission intensity of Ar I 750.4 nm and 811.5 nm. These emission intensities oscillate at f_{AM}. The 750.4 nm emission intensity is high around t = 3 s around the plasma/sheath boundaries near the powered and grounded electrode, whereas the 811.5 nm emission intensity is rather low around t = 3 s. Both intensities at t = 7 s are higher than those at t = 3 s. The 750.4 nm emission takes place due to the direct excitation:

$Ar + e \rightarrow Ar(4p'[1/2]0) + e\ (\varepsilon \geq 13.48eV)$,

$Ar(4p'[1/2]0) \rightarrow Ar(4s'[1/2]1) + h\nu\ (750.4nm)$.

Ar I 811.5 nm is emitted by the two step excitation:

$Ar + e \rightarrow Ar_m(4s[3/2]2) + e\ (\varepsilon \geq 11.55eV)$,

$Ar_m + e \rightarrow Ar(4p[5/2]3) + e\ (\varepsilon \geq 1.53eV)$, and

$Ar(4p[5/2]3) \rightarrow Ar_m(4s[3/2]2) + h\nu\ (811.5nm)$.

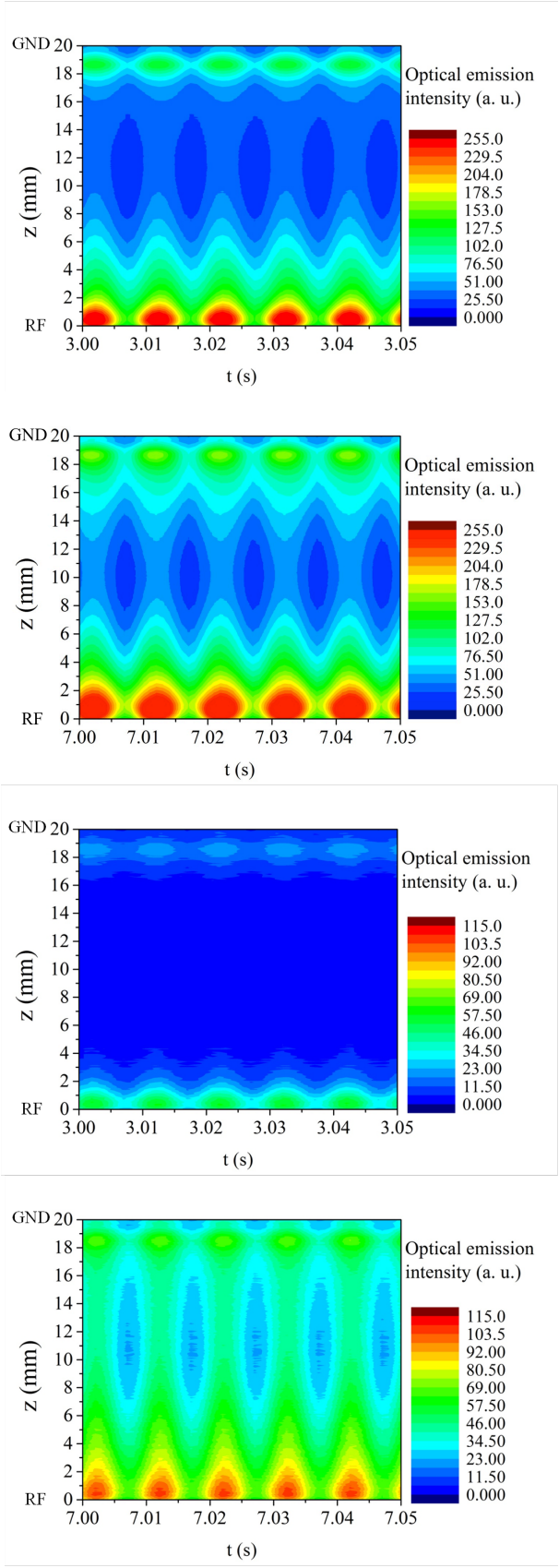

Fig. 3. Time evolution of the spatial profiles of optical emission intensity of 750.4 nm during (a) t = 3-3.05 s, (b) t = 7-7.05 s and that of 811.5nm during (c) t = 3-3.05 s, (d) t = 7-7.05 s.

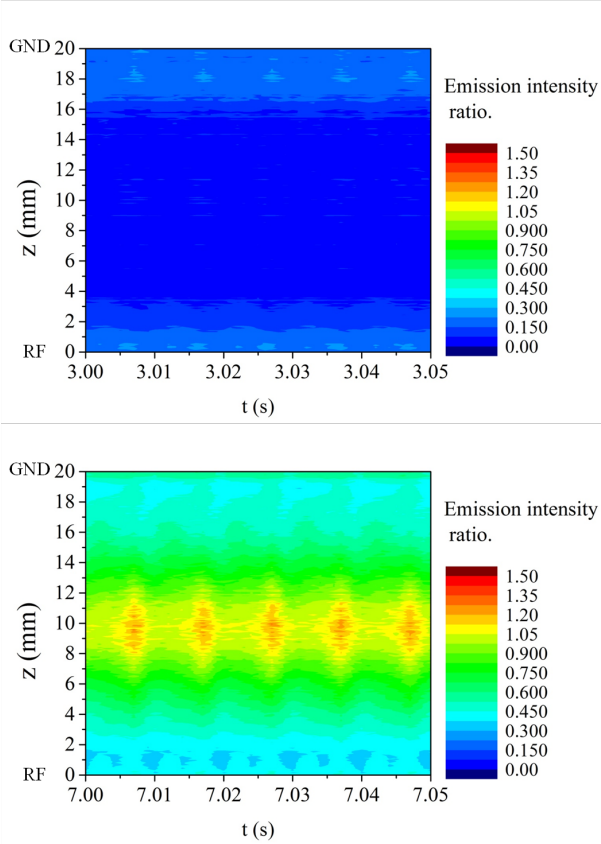

Fig. 4. Time evolution of the spatial profiles of optical emission intensity ratio during (a) t = 3-3.05 s, (b) t = 7-7.05 s.

The intensity ratio of 811.5nm to 750.4nm gives information on Ar metastable density [16-17]. We have employed the ratio as an indicator of radical density. Figures 4(a) and 4(b) show time evolution of the spatial profile of the ratio. The ratio increases with t around z= 10 mm in the plasma bulk between the powered and grounded electrodes. The emission intensity ratio oscillates at f_{AM}.These results suggest that Ar metastable density is modulated by AM. It should be noted that the emission intensities and their ratio have no phase delay as in Fig. 2.

Nonlinear coupling between plasmas and nonoparticles is suggested by the power spectra of LLS intensity. Figure 5 shows a spatial profile of power spectrum of the LLS intensity. The power spectrum was normalized at the AM frequency. The peaks of fluctuation of the LLS intensity are observed at f_{AM} and its higher harmonics. It suggests perturbation of LLS intensity is coupled with AM of the discharge voltage. In addition, perturbations at subharmonics such as $f = 3/5f_{AM}$ = 60Hz are observed in Fig. 5. We also obtained power spectra of the optical emission intensities and their ratio. They are perturbed at f_{AM} and its higher harmonics, whereas no peaks at subharmonics are observed. These results suggest that the amount of nanoparticles is nonlinearly coupled with the radical density.

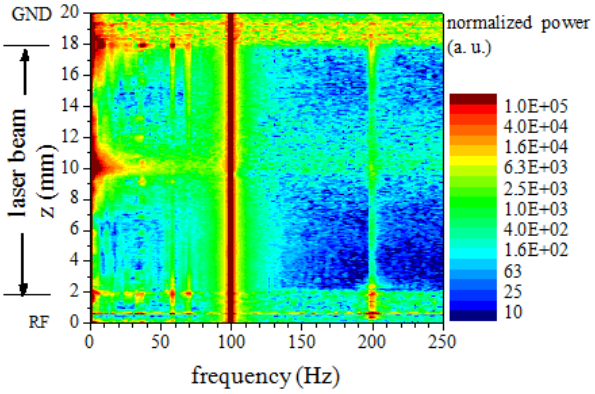

Fig. 5. Spatial profile of power spectrum of the LLS

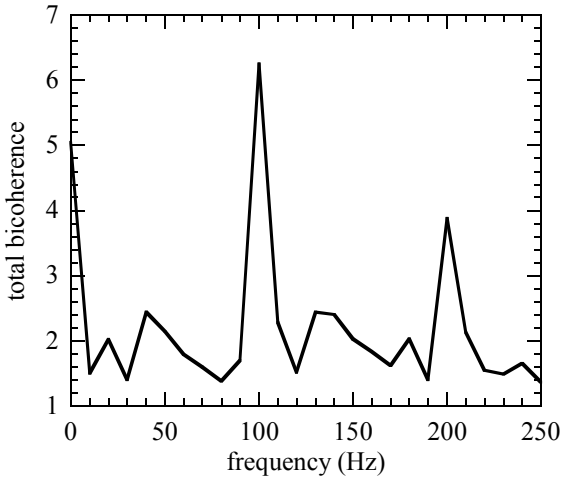

Fig. 6. Total bicoherence of the LLS intensity at z = 4 mm.

Bispectrum analysis of the LLS intensity was performed in order to understand the origins of subharmonics of power spectra and nonlinear coupling between plasmas and nanoparticles. The bispectrum analysis brings about fruitful results in the field of plasma turbulence [18-20]. Bicoherence revelas a correlation among three frequencies, f_1, f_2, and f_3. It is close to 1 when $f_1 + f_2 = f_3$; it is close to 0 without such relation [21]. The squared bicoherence is defined as

$$b^2(f_1, f_2) = \frac{|\langle \varphi^*(f_3)\varphi(f_1)\varphi(f_2)\rangle|^2}{\langle|\varphi(f_3)|^2\rangle\langle|\varphi(f_1)\varphi(f_2)|^2\rangle}, \qquad (1)$$

where φ is the Fourier component. The total bicoherence which indicates the total impact of fluctuation at f_3 is defined as

$$B^2(f_3) = \sum_{f_1+f_2=f_3} b^2(f_1, f_2). \qquad (2)$$

Figure 6 shows the total bicoherence of LLS intensity at z=4 mm above the center of the powered electrode. The peaks of total bicoherence from LLS intensity are observed at f_{AM} and its higher harmonics. In addition, nonlinear coupling is observed in a frequency range of 40-60 Hz which corresponds to the subharmonics of power spectrum of LLS intensity.

Based on our theoretical prediction [11], it indicates that nonlinear coupling between nanoparticles and radicals leads to the pertubations at subharmonics. Thus, bispectrum analysis is useful for shedding light on interactions between plasmas and nano-materials.

4. Conclusion

We have analysed fluctuation of nanoparticle amount in amplitude modulated capacitive-ly-coupled discharge plasmas. The power spectra of LLS intensity show some peaks at subharmonics of AM frequency. The total bicoherence of LLS intensity shows that nanoparticles are nonlinearly coupled with radical density. Therefore, the perturbation at subharmonics of AM frequency is caused by non-linear coupling between nanoparticles and radicals.

Acknowledgment

This work was partly supported by JSPS KA-KENHI grant number 26246036.

References

[1] M. Meyyappan, et al., J. Phys. D, **44** (2011) 174002.
[2] M. Shiratani, et al., J. Phys. D, **44** (2011) 174038.
[3] Y. Watanabe, et al., Appl. Phys. Lett. , **53** (1988) 1263.
[4] M. Shiratani, et al., J. Appl. Phys., **79** (1996) 104.
[5] M. Shiratani, et al., Jpn. J. Appl. Phys., **39** (2000) 287.
[6] K. Koga, et al., Appl. Phys. Lett. , **77** (2000) 196.
[7] K. Koga, et al., J. Phys. D, **40** (2007) 2267.
[8] K. Kamataki, et al., Appl. Phys. Express, **4** (2011) 105001.
[9] K. Kamataki, et al., Thin Solid FIlms., **518** (2009) 6492.
[10] K. Kamataki, et al., J. Inst., **7** (2012) C04017.
[11] M. Shiratani, et al., Jpn. J. Appl. Phys., **53** (2014) 010201.
[12] M. Shiratani, et al., Faraday Discussions., **137** (2008) 127.
[13] S. Nunomura, et al., Phys. Plasmas, **15** (2008) 080703.
[14] S. Iwashita, et al., Jpn. J. Appl. Phys., **47** (2008) 6875.
[15] M. Shiratani, et al., JPS Conf. Ser., **1** (2014) 5083.
[16] T. Czerwiec and D. B. Graves. J.Phys. , D, **37** (2004) 2827.
[17] A. M. Daltrini, et al., JICS, **67** (2007).
[18] Y. Nagashima, et al., Rev. Sci. Instrum., **77** (2006) 045110.
[19] T. Kobayashi, et al., Phys. Rev. Lett. **111** (2013) 035002.
[20] S. Inagaki, et al., Nucl. Fusion, **54** (2014) 114014.
[21] B. Ph. van Milligen, et al., Phys. Plasmas, **2** (1995) 3017.